AFRL-SN-RS-TR-1999-168
Final Technical Report
August 1999

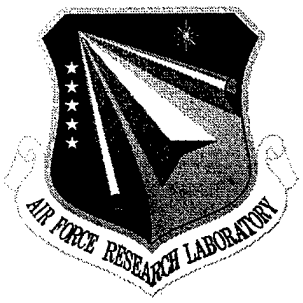

APPLICATIONS OF PHOTOREFRACTIVE AND RESONANT SYSTEMS TO OPTICAL SIGNAL PROCESSING

Tufts University

Mark Cronin-Golomb and Venkatapuram S. Sudarshanam

APPROVED FOR PUBLIC RELEASE; DISTRIBUTION UNLIMITED.

AIR FORCE RESEARCH LABORATORY
SENSORS DIRECTORATE
ROME RESEARCH SITE
ROME, NEW YORK

This report has been reviewed by the Air Force Research Laboratory, Information Directorate, Public Affairs Office (IFOIPA) and is releasable to the National Technical Information Service (NTIS). At NTIS it will be releasable to the general public, including foreign nations.

AFRL-SN-RS-TR-1999-168 has been reviewed and is approved for publication.

APPROVED: Philip R. Hemmer

PHILIP R. HEMMER
Project Engineer

FOR THE DIRECTOR: Robert V. McGahan

ROBERT V. McGAHAN, Technical Advisor
Electromagnetics Technology Division
Sensors Directorate

If your address has changed or if you wish to be removed from the Air Force Research Laboratory Rome Research Site mailing list, or if the addressee is no longer employed by your organization, please notify AFRL/SNHC, 80 Scott Drive, Hanscom AFB MA 01731-2909. This will assist us in maintaining a current mailing list.

Do not return copies of this report unless contractual obligations or notices on a specific document require that it be returned.

REPORT DOCUMENTATION PAGE	Form Approved OMB No. 0704-0188

1. AGENCY USE ONLY *(Leave blank)*	2. REPORT DATE	3. REPORT TYPE AND DATES COVERED
	August 1999	Final May 96 - May 98

4. TITLE AND SUBTITLE
APPLICATIONS OF PHOTOREFRACTIVE AND RESONANT SYSTEMS TO OPTICAL SIGNAL PROCESSING

5. FUNDING NUMBERS
C - F30602-96-2-0101
PE - 62702F
PR - 4600
TA - 19
WU - P8

6. AUTHOR(S)
Mark Cronin-Golomb and Venkatapuram S. Sudarshanam

7. PERFORMING ORGANIZATION NAME(S) AND ADDRESS(ES)
Tufts University
Contracts & Grants Administration
Packard Hall
Medford MA 02155

8. PERFORMING ORGANIZATION REPORT NUMBER
N/A

9. SPONSORING/MONITORING AGENCY NAME(S) AND ADDRESS(ES)
Air Force Research Laboratory/SNHC
80 Scott Drive
Hanscom AFB MA 01731-2909

10. SPONSORING/MONITORING AGENCY REPORT NUMBER
AFRL-SN-RS-TR-1999-168

11. SUPPLEMENTARY NOTES
Air Force Research Laboratory Project Engineer: Philip Hemmer/SNHC/(781) 377-5170

12a. DISTRIBUTION AVAILABILITY STATEMENT
Approved for public release; distribution unlimited.

12b. DISTRIBUTION CODE

13. ABSTRACT *(Maximum 200 words)*

The experiments done in this grant can be broadly classified into two stages. The goal of both these stages was to demonstrate all-optical high-speed turbulence aberration correction through nonlinear optical phase conjugation. The first stage involved the development of a phase conjugate mirror (PCM) based on non-degenerate four-wave-mixing (NDFWM). Coherent population trapping (CPT) in sodium vapor permitted the use of low intensity cw lasers. The second stage involved the development of a phase conjugate resonator (PCR) that could correct intracavity aberrations. In comparison to the PCM using CPT, the PCR was also based on CPT but was degenerate in optical frequency, with a simpler experimental set-up. A high conjugate power gain exceeding 35 was achieved in both the non-degenerate and degenerate FWM configurations. High gain is of importance in applications involving wide apertures. Experiments were demonstrated using a helium jet in air operated at a frequency of 18kHz with flow speeds up to 250m/s. Substantial reduction in the modulation depth of temporal aberration is shown for both the PCM and PCR cases, along with high-fidelity spatial aberration correction.

14. SUBJECT TERMS
Optical Phase Conjugation, Raman Effect, Coherent Population Trapping

15. NUMBER OF PAGES
16

16. PRICE CODE

17. SECURITY CLASSIFICATION OF REPORT	18. SECURITY CLASSIFICATION OF THIS PAGE	19. SECURITY CLASSIFICATION OF ABSTRACT	20. LIMITATION OF ABSTRACT
UNCLASSIFIED	UNCLASSIFIED	UNCLASSIFIED	UL

Summary:
The experiments done in this period can be broadly classified into two stages. The goal of both these stages was to demonstrate all-optical high-speed turbulence aberration correction through nonlinear optical phase conjugation. The first stage involved the development of a phase conjugate mirror (PCM) based on non-degenerate four-wave-mixing (NDFWM). Coherent population trapping (CPT) in sodium vapor permitted the use of low-intensity cw lasers. The second stage involved the development of a phase conjugate resonator (PCR) that could correct intracavity aberrations. In comparison to the PCM using CPT, the PCR was also based on CPT but was degenerate in optical frequency, with a simpler experimental set-up. A high conjugate power gain exceeding 35 was achieved in both the non-degenerate and degenerate FWM configurations. High gain is of importance in applications involving wide apertures. Experiments were demonstrated using a helium jet in air operated at a frequency of 18 kHz with flow speeds up to 250 m/s. Substantial reduction in the modulation depth of temporal aberrations is shown for both the PCM and PCR cases, along with high-fidelity spatial aberration correction.

First Stage: the nondegenerate PCM :
Conventional aberration correction is based on the use of adaptive optic systems that use a two-step approach of optically sensing the wavefront and actively (electronically) correcting the wavefront error. Such adaptive optic systems can correct for turbulence aberrations in the atmospheric propagation regime, at speeds up to 300 Hz. However, in the aero-optical regime of turbulence, the required bandwidth[1] is up to 100 kHz. Long ago,[2] it was suggested that all-optical phase conjugation should be capable of correcting aberrations due to turbulence. However, most existing nonlinear optical materials, for example, photorefractive media[3] have a sufficiently fast response only if high power pump beams are used. Real-time compensation of atmospheric turbulence using four-wave mixing (FWM) in sodium (Na) vapor with cw lasers of 20W/cm^2 was demonstrated earlier.[4] However, the conjugate gain was only 0.2. In the first stage, we demonstrate the use of cw lasers with low intensities of the order of 5W/cm^2 to perform high speed spatio-temporal aberration correction and still achieve a high phase conjugate gain of 32.
Previously, we reported[5] a high conjugate gain with a response faster than 1 μs employing Gaussian beams and low pump intensities of ~1 W/cm^2. This was achieved in an externally pumped FWM configuration utilizing the mechanism of coherent population trapping [5-9] (CPT) in Na vapor. Such low pump intensities could be used because the optical nonlinearity saturates at an intensity below that needed to saturate the optical transition. Here we show that this performance does not degrade in the presence of large angle aberrations caused by a turbulent jet flow.
The experimental arrangement, method and results are discussed in Ref.[10], and are also reported in our Annual Report for the period ending May 1, 1997.

Second Stage: the degenerate PCR

By the addition of a highly reflective mirror, a high-gain PCM can be modified to resonate as a cavity and generate a high-fidelity optical output that has several interesting characteristics.[2] Such a phase conjugate resonator (PCR) has many applications ranging from aberration correction and target / source tracking to associative memories, optical data processing, imaging threshold detectors, and one-way image transmission (when used in combination with a phase conjugate mirror, PCM)[2,11,12]. The practicality of PCM's for these applications depends strongly on the requirements of the nonlinear optic material. Resonant systems, such as sodium vapor are often preferred because they provide gain greater than unity and a response time in the nanosecond regime, even with cw lasers. However, previous Na vapor PCR's required high intensity pump beams, which necessitated strong focussing to spot sizes of ~ 100μm[13]. This limits applications, especially those related to imaging. In this paper, we demonstrate a PCR that has a 320 times lower resonating threshold (~4.5 W/cm^2 pump intensity) than the best previous[13] Na vapor PCR. This low threshold intensity allows large diameter pump beams to be used and has permitted, for the first time, demonstration of a PCR with fast intracavity aberrations.

Non-degenerate four-wave mixing (NDFWM) based on Raman coherent population trapping (CPT) between hyperfine sublevels in Na vapor was shown previously[10] to correct turbulence aberrations in a PCM geometry. In order to demonstrate a single-frequency PCR using NDFWM, the frequencies of the 'probe' and 'conjugate' beams have to be matched. In principle, frequency matching can be accomplished by using Raman CPT between degenerate Zeeman sublevels. However, previous attempts to demonstrate a PCR based on Zeeman coherence have been unsuccessful. For example, in Ref.[13], DFWM based on Zeeman coherence was found to be less efficient than the population grating mechanism. In Ref.[14], a resonator with cross polarized pump and probe beams was investigated. This was based on a maximum gain of 3.5 for a pump intensity of 1.4 kW/cm^2 and detuning of 4.5 GHz from the Na D_1 transition. However, this gain value included contribution from a phase-matched distributed feedback term making the resonator unsuitable for operation as a PCR with an intracavity aberrator.

In the PCR experimental arrangement shown in Fig.1, the linearly polarized forward (F) and backward (B) pump beams counterpropagate in the Na vapor cell. The pumps are slightly focused by lenses, L, (f = 1m) to a FWHM diameter of 660 μm at the cell center. An optical isolator, I, prevents feedback into the dye laser from reflections. A PCR cavity is formed between the high-reflectivity (95%) output coupler, R, and the Na vapor high-gain PCM. To resonate efficiently, light reflected from the ordinary mirror R must be a plane wave. However, this plane wave will be aberrated (beam A) after passing through the helium jet and so must be phase conjugated in the Na cell to produce a corrected beam C after passing back through the helium jet. The portion of A transmitted through the cell is denoted by 'T'. In the degenerate Na PCM, the conjugate beam is generated primarily by the scattering of B from the grating formed by F and A. The DFWM interaction excites Raman transitions among Na magnetic sublevels. This gives a PCR beam that is nominally cross-polarized relative to both F and B. Because of this cross-polarization, polarizing beam splitters, PBS, can be used to facilitate the

steering of A into the cell, and to better separate C from B. The PBS's are not required to

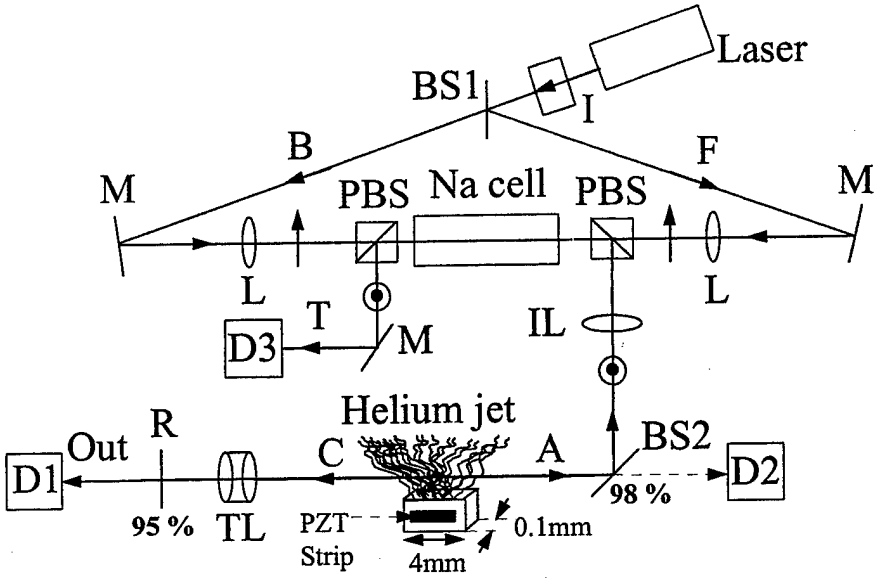

Fig.1. Schematic of the experimental arrangement for a degenerate PCR with intracavity turbulence aberration correction.

operate the PCR or maintain cross-polarization between the pumps and PCR beams. The PCR beams A and C are aligned to intercept F and B in the cell at a vertical angle of ~ 8.5 mrad. In the absence of turbulence, beam A (and C) has a diameter of ~ 0.23mm at the center of the cell. A telescope, TL, compensates diffraction effects in the PCR cavity. The typical optical intensity of F and B at the cell center is about 10 W/cm^2 each, unless otherwise stated. The intensity of C (or A) at the cell center is estimated to be ~ 2.6 W/cm^2 at the maximum intracavity PCR power of 1.7 mW. The Na vapor cell is a heat-pipe oven operated at ~ 260°C with an ambient pressure of ~ 18 mTorr. No buffer gas is added to the cell. Stray magnetic fields are reduced to less than 20 mG with the use of magnetic shielding around the cell.

The turbulent jet is placed 1m away from the imaging lens, IL, (f = 25cm) which images it into the cell with a demagnification of ~67%. This jet is obtained by forcing helium gas at room temperature through a rectangular nozzle (4mm x 0.1mm) placed ~ 3mm below the PCR beam path. The nozzle is acoustically driven by a PZT transducer at the flow resonance frequency of 17.8 kHz. The average helium flow speed at the nozzle exit is estimated to be ~ 250m/s.

To demonstrate spatial aberration correction, the profile of C is sampled by the CCD camera (D1) and the profile of A is sampled by D2. The D1 camera is placed 1.92 m away from the jet, and D2 is 0.57m away from the jet. Temporal aberration is measured by replacing D1 (and D2) by a 0.3mm pinhole mounted on a photodetector(PPD). The transverse location of the PPD is adjusted for maximum

amplitude of the 17.8 kHz intensity variation caused by the turbulence. The ratio of the peak-to-peak intensity variation to the maximum intensity level is defined as the modulation depth. This allows an intensity-independent comparison of the temporal aberrations in beams C and A.

Spatial aberration correction is demonstrated in Fig.2 through (time-averaged) CCD images. The beam profiles are shown both as two-dimensional contour plots at intervals of 20% of the peak intensity, and as one-dimensional line traces made near the vertical center of each profile. The profile of A, sampled by D2, is shown in Fig.2(a) with the helium flow ON and OFF (left and right profiles respectively), while that of C, sampled by D1 is shown in Fig.2(b) under corresponding flow conditions. As seen from Figs.2(a) and 2(b), a well-corrected nearly-circular spot is seen at the output coupler R on double-pass through the jet, whereas A is severely aberrated by the helium jet. The difference in the sizes of the beams C and A shown in Fig.2 is due to the magnification by the telescope, TL. The profile of the transmitted PCR beam, T, is sampled by camera

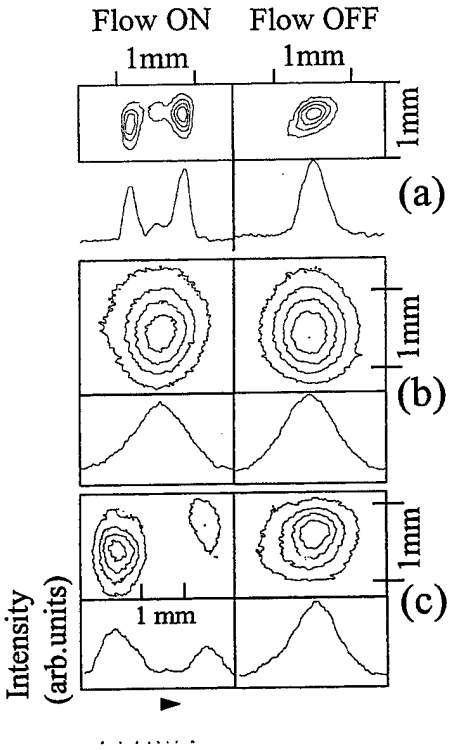

Fig.2. Data showing spatial aberration correction: 2-D contours (upper plots) and 1-D line traces (lower plots) of the intensity profile of (a) the aberrated PCR beam, A, (b) the compensated PCR beam, C, and (c) the transmitted PCR beam, T. Contour lines are drawn at 80, 60, 40 and 20 % of peak intensity.

D3 which is 0.54 cm away from the cell center (see Fig.1) and is shown in Fig.2(c) with the flow ON and OFF. As expected, T is aberrated by the flow in like manner to A. The helium flow reduced the intracavity PCR power to half its value without flow.

Fast temporal aberration correction at 17.8 kHz is demonstrated in Fig.3 through plots of the instantaneous output voltage from the PPD. Here, Fig.3(a) shows the effect of turbulence on the aberrated PCR beam A, while Fig.3(b) shows that for the compensated PCR beam, C. From this data, the signal modulation depth in A is estimated at ~63.6% whereas that in C is ~6.6%, demonstrating that temporal aberrations are corrected by a factor of ~9.6 in the PCR beam near R.

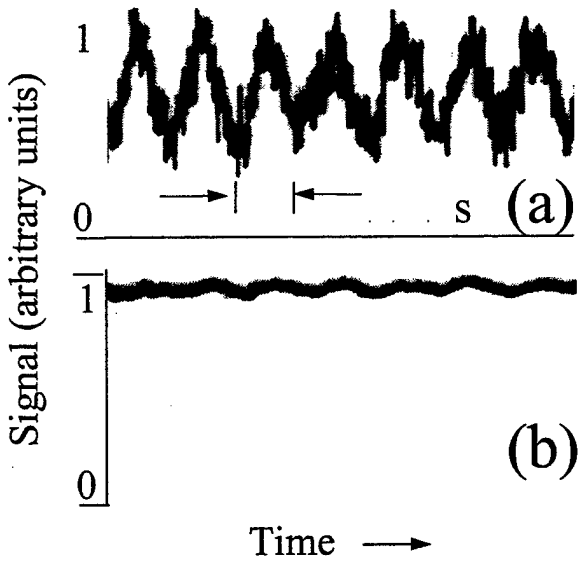

Fig.3. Temporal aberration correction: PPD signal showing turbulence effects on (a) aberrated PCR beam, A, and (b) the compensated PCR beam, C.

In order to establish that the system is indeed based on purely DFWM and not NDFWM as in Ref.[10], the optical frequency of C (and A) is determined by beating with a probe beam, P (not shown in Fig.1) that is shifted by 5 MHz relative to F. Figure 4(a) shows the output frequency spectrum of an avalanche photodiode (APD) on which the two beams C (or A) and P are beat. Figure 4(b) shows the electrical spectrum of the two AOM drive signals. The agreement between the optical and electrical frequency shifts in Figs.4(a) and (b) establishes that DFWM indeed gives rise to C and A. The single PCR peak seen from Fig.4(a) shows that the PCR is oscillating in a single longitudinal mode even without any intracavity frequency-selective elements. For the cavity length of 2.1 m, the expected[11] PCR longitudinal mode spacing (c/4L) is ~36 MHz. Multiple longitudinal modes are not supported in our PCR because the two-photon bandwidth of the CPT interaction is far less, as discussed later.

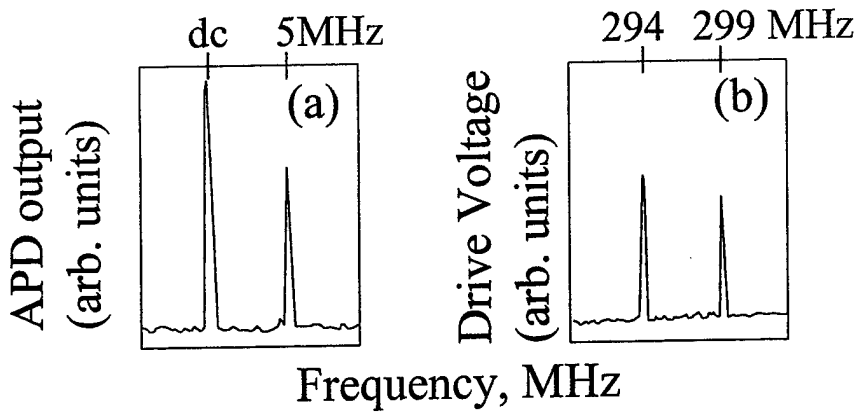

Fig.4. Verification of DFWM: (a) the optical beat between C (or A) and the probe P (shifted by 5 MHz from F), and (b) the electrical voltage spectrum of the two AOM drive signals at 294 and 299 MHz used to generate P.

Figure 5(a) shows the intracavity optical power as a function of the pump frequency. The peaks named I, J and K can be selectively enhanced in power at their respective frequencies by changing the alignment angle between C (A) and the pumps F and B. Aberration correction measurements described in this paper are done with the peak I enhanced as it occurs at the largest angle of ~ 8.5 mrad from the pumps. This also avoids the conical emission[13,15] that occurs near the peak K. The conical emission near peak K has a typical half-angle of ~ 5mrad and has a characteristic hexagonal pattern. The small broadened peaks between J and K are from diffuse conical emission that is primarily orthogonal in polarization to C (and A). The peak I is enhanced when the pump laser frequency is red-detuned by ~300 MHz from the F=2 to the F' =1 transition. It should be noted that the Doppler width of Na vapor at 260°C is ~ 1.1 GHz. Therefore, the detuning measured applies only to the zero-velocity group in the vapor.

The threshold pump intensity at which the PCR output becomes unstable in time was determined (with the flow OFF) by attenuating the total pump power obtained from the laser. The laser frequency was kept fixed at the peak I shown in Fig.5(a). The threshold intensity for each pump was found to be 4.5W/cm^2.

To test for CPT, a probe beam, P, with variable frequency relative to F is conjugated, with the output coupler R misaligned to stop oscillation of the PCR. However, other experimental operating conditions remain unchanged. The pump laser is tuned to the peak I and the difference frequency, Δf, between P and F is varied using the set of two AOM's described earlier. Figure 5(b) shows the conjugate power gain (probe

power ~90 μW) as a function of the difference frequency between F and P, for two

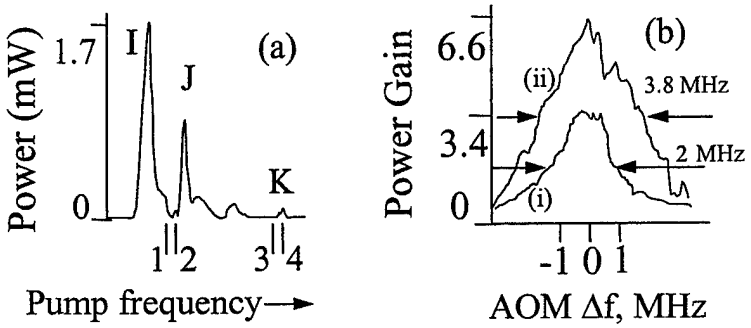

Fig.5. (a) PCR intracavity power as a function of the pump frequency. The numbers 1 through 4 correspond to the following D_1 transitions: (1) F=2 ↔ F′=1 (2) F=2 ↔ F′=2 (3) F=1 ↔ F′=1, and (4) F=1 ↔ F′=2. (b) The PCM conjugate gain as a function of Δf for the two pump intensities (i) 4.6 W/cm^2 and (ii) 10 W/cm^2.

different pump intensities. The FWHM of the gain is ~2 MHz for the lower pump intensity, which is far less than the 10 MHz excited state decay rate of Na. This subnatural difference-frequency linewidth for the two-photon interaction is taken as direct evidence for Raman CPT. Another test[7-10] for Raman CPT is the dependence of the FWHM on the generalized two-photon Rabi frequency (which is proportional to pump intensity). The linewidth increases from 2 MHz to 3.8 MHz when the pump intensity increases from 4.6 W/cm^2 to 10 W/cm^2. In order to test the double-Λ nature of the CPT-based DFWM interaction,[10] the conjugate and the probe beams are beat on an APD. When P is shifted by 1MHz from F (and B), the conjugate beam is found shifted by 2 MHz from P, and by 1 MHz from F (and B).

Conclusion:

In conclusion, a low-threshold PCR based on DFWM involving a double-Λ CPT interaction has been presented. Temporal aberrations caused by intracavity turbulence driven at 18 kHz with a flow speed of 250m/s have been corrected by a factor of 9.6. Recently,[16] potential applications such as frequency standards, intracavity spectroscopy, and optical magnetometry have been proposed for intracavity CPT.

References:

1. R. J. Hugo and E. J. Jumper, Appl. Opt. **35**, 4436 (1996).
2. See, for example, R. A. Fisher, ed., *Optical Phase Conjugation* (Academic, New York, 1983), chapters 13 and 14.
3. See, for example, B. Monson, G. J. Salamo, A. G. Mott. M. J. Miller, E. J. Sharp, W. W. Clark III, G. L. Wood, and R. R. Neurgaonkar, Opt. Lett. **15**, 12 (1990).
4. R. C. Lind and G. J. Dunning, Laser Focus / Electro-Optics **19**, 14 (1983).
5. P. R. Hemmer, D. P. Katz, J. Donoghue, M. Cronin-Golomb, M. S. Shahriar and P. Kumar, Opt. Lett. **20**, 982 (1995).
6. G. Alzetta, A. Gozzini, L. Moi, and G. Orriols, Nuovo Cimento B **36**, 5 (1976).
7. H. R. Gray, R. M. Whitley, and C. R. Stroud, Opt. Lett. **3**, 218 (1978); E. Arimondo, in *Progress in Optics XXXV*, E. Wolf, ed. (Elsevier, New York, 1996), pp.258- 354.
8. P. M. Radmore and P. L. Knight, J. Phys. B **15**, 3405 (1982).
9. J. Donoghue, M. Cronin-Golomb, J. S. Kane, and P. R. Hemmer, Opt. Lett. **16**, 1313 (1991).
10. V. S. Sudarshanam, M. Cronin-Golomb, P. R. Hemmer and M. S. Shahriar, Opt.Lett. **22**, 1141 (1997).
11. R. C. Lind and D. G. Steel, Opt. Lett. **6**, 554 (1981).
12. A. Yariv and S. -K. Kwong, Opt. Lett. **11**, 186 (1986); G. J. Dunning, S. W. McCahon, M. B. Klein, and D. M. Pepper, J. Opt. Soc. Am. **B 11**, 339 (1994); M. B. Klein, G. J. Dunning, G. C. Valley, R. C. Lind, and T. R. O'Meara, Opt. Lett. **11**, 575 (1986).
13. J. R. R. Leite, P. Simoneau, D. Bloch, S. Le Boiteux and M. Ducloy, Europhys. Lett. **2**, 747 (1986).
14. M. Vallet, M. Pinard and G. Grynberg, Opt. Comm. **81**, 403 (1991).
15. G. Grynberg, E. Le Bihan, P. Verkerk, P. Simoneau, J. R. R. Leite, D. Bloch, S. Le Boiteux and M. Ducloy, Opt. Commun. **67**, 363, (1988).
16. M. D. Lukin, M. Fleischhauer, M. O. Scully, and V. L. Velichansky, Opt. Lett. **23**, 295 (1998).